[1] a) S. Rowan, D. E. Fisher, *Leukemia* **1997**, *11*, 457 – 465; b) P. H. Krammer, *Adv. Immunol.* **1998**, *71*, 164 – 210; c) A. Ashkenazi, V. M. Dixit, *Science* **1998**, *281*, 1305 – 1308; d) P. Wehrli, I. Viard, R. Bullani, J. Tschopp, L. E. French, *J. Invest. Dermatol.* **2000**, *115*, 141 – 148; e) T. Herget, *Nachr. Chem. Tech. Lab.* **2001**, *49*, 328 – 330; f) U. Sartorius, I. Schmitz, P. H. Krammer, *ChemBioChem* **2001**, *2*, 20 – 29.
[2] A. M. Danen-Van Oorschot, D. F. Fischer, J. M. Grimbergen, B. Klein, S.-M. Zhuang, J. H. F. Falkenburg, C. Backendorf, P. H. A. Quax, A. J. Van der Eb, H. M. Noteborn, *Proc. Natl. Acad. Sci. USA* **1997**, *94*, 5843 – 5847.
[3] a) Y. Hayakawa, J. W. Kim, H. Adachi, K. Shin-ya, K. Fujita, H. Seto, *J. Am. Chem. Soc.* **1998**, *120*, 3524 – 3525; b) J. W. Kim, H. Adachi, K. Shin-ya, Y. Hayakawa, H. Seto, *J. Antibiot.* **1997**, *50*, 628 – 630.
[4] a) A. R. Salomon, Y. Zhang, H. Seto, C. Khosla, *Org. Lett.* **2001**, *3*, 57 – 59; b) A. R. Salomon, D. W. Voehringer, L. A. Herzenberg, C. Khosla, *Chem. Biol.* **2001**, *8*, 71 – 80.
[5] a) J. Schuppan, B. Ziemer, U. Koert, *Tetrahedron Lett.* **2000**, *41*, 621 – 624; b) K. C. Nicolaou, Y. Li, B. Weyershausen, H.-X. Wei, *Chem. Commun.* **2000**, 307 – 308; c) G. A. Sulikowski, W.-M. Lee, B. Jin, B. Wu, *Org. Lett.* **2000**, *2*, 1439 – 1442.
[6] Since the hydroxy group at C20 is sterically hindered, lactonization should occur with the hydroxy group at C19. See also: a) R. B. Woodward, E. Logusch, K. P. Nambiar, K. Sakan, D. E. Ward, B.-W. Au-Yeung, P. Balaram, L. J. Browne, P. J. Card, C. H. Chen, R. B. Chênevert, A. Fliri, K. Frobel, H.-J. Gais, D. G. Garratt, K. Hayakawa, W. Heggie, D. P. Hesson, D. Hoppe, I. Hoppe, J. A. Hyatt, D. Ikeda, P. A. Jacobi, K. S. Kim, Y. Kobuke, K. Kojima, K. Krowicki, V. J. Lee, T. Leutert, S. Malchenko, J. Martens, R. S. Matthews, B. S. Ong, J. B. Press, T. V. Rajan Babu, G. Rousseau, H. M. Sauter, M. Suzuki, K. Tatsuta, L. M. Tolbert, E. A. Truesdale, I. Uchida, Y. Ueda, T. Uyehara, A. T. Vasella, W. C. Vladuchick, P. A. Wade, R. M. Williams, H. N.-C. Wong, *J. Am. Chem. Soc.* **1981**, *103*, 3213 – 3215; b) M. Kageyama, T. Tamura, M. H. Nantz, J. C. Roberts, P. Somfai, D. C. Whritenour, S. Masamune, *J. Am. Chem. Soc.* **1990**, *112*, 7407 – 7408.
[7] B. Tse, *J. Am. Chem. Soc.* **1996**, *118*, 7094 – 7100.
[8] B. H. Lipshutz, R. Keil, E. L. Ellsworth, *Tetrahedron Lett.* **1990**, *31*, 7257 – 7260.
[9] Bromide **11** was prepared from the corresponding alcohol as follows: 1) MsCl, Et_3N, 2) LiBr, acetone (Ms = mesyl = methanesulfonyl). See: V. Fargeas, P. L. Mênez, I. Berque, J. Ardisson, A. Pancrazi, *Tetrahedron* **1996**, *52*, 6613 – 6634.
[10] M. T. Reetz, *Angew. Chem.* **1984**, *96*, 542 – 555; *Angew. Chem. Int. Ed. Engl.* **1984**, *23*, 556 – 569.
[11] M. Larcheveque, S. Henrot, *Tetrahedron* **1987**, *43*, 2303 – 2310.
[12] D. B. Dess, J. C. Martin, *J. Org. Chem.* **1983**, *48*, 4155 – 4156.
[13] K. Takai, T. Ichiguchi, S. Hisaka, *Synlett* **1999**, *8*, 1268 – 1270.
[14] The light sensitivity of **18** is under current investigation. Upon irradiation at 365 nm, the absorption band at 295 nm decreased. Concomittantly an increase at about 240 nm is observed.
[15] a) J. K. Stille, *Angew. Chem.* **1986**, *98*, 504 – 519; *Angew. Chem. Int. Ed. Engl.* **1986**, *25*, 508 – 523; b) T. N. Mitchell, *Synthesis* **1992**, 803 – 815; c) I. Paterson, V. A. Doughty, M. D. McLeod, T. Trieselmann, *Angew. Chem.* **2000**, *39*, 1364 – 1368; *Angew. Chem. Int. Ed.* **2000**, *39*, 1308 – 1312.
[16] a) G. D. Allred, L. S. Liebeskind, *J. Am. Chem. Soc.* **1996**, *118*, 2748 – 2749; b) I. Paterson, H.-G. Lombart, C. Allerton, *Org. Lett.* **1999**, *1*, 19 – 22.
[17] a) J. Inanaga, K. Hirata, H. Saeki, T. Katsuki, M. Yamaguchi, *Bull. Chem. Soc. Jpn.* **1979**, *52*, 1989 – 1993; b) D. A. Evans, D. M. Finch, T. E. Smith, V. J. Cee, *J. Am. Chem. Soc.* **2000**, *122*, 10033 – 10046.
[18] Analytical data (R_f and $[\alpha]_D$ values, IR, ^1H and ^{13}C NMR, and HR mass spectra) of **12**, **18**, **20**, **21**, and apoptolidinone are available in the Supporting Information.

Carbon Nanofilaments in Heterogeneous Catalysis: An Industrial Application for New Carbon Materials?**

Gerhard Mestl, Nadezhda I. Maksimova, Nicolas Keller, Vladimir V. Roddatis, and Robert Schlögl*

The direct dehydrogenation of ethylbenzene to styrene is one of the ten most important industrial processes. In this process a potassium-promoted iron catalyst is used at temperatures between 870 and 930 K.[1] However, this method is thermodynamically limited and, because of the required excess of steam, very energy consuming.[2, 3] The oxidative dehydrogenation (ODH) of ethylbenzene could be a promising alternative in which the hydrogen generated is directly oxidized making the overall process exothermic.

Mechanistic studies of the dehydrogenation of ethylbenzene on single-crystal model surfaces provide fundamental information about the role of the active K – Fe phase.[4–7] This surface is evidently well suited to generate a graphitic carbon deposit. Therefore, it is possible that these carbon deposits are actually the catalytically active phase.

Transition metal oxides[8] and phosphates[9, 10] as well as polymers[11] have been described as active and selective catalysts for the ODH of ethylbenzene. The carbon deposits[12] detected on such catalysts again point to an active role of carbon in this reaction. Accordingly, catalytic activity in the ODH was demonstrated for activated charcoals,[13, 14] their commercialization however, is impossible because of their low oxidation resistance.[15] Graphite, on the other hand, exhibits activity in the ODH of methanol.[16] Thus, graphitic carbon materials, that is, nanofilaments with high surface area, are promising candidates for dehydrogenation catalysts in the presence of oxygen.

We have tested the catalytic properties of lamp soot, graphite, and nanofilaments for the ODH of ethylbenzene to styrene. Figure 1 displays the catalytic properties of the investigated carbon materials with time on stream *t*. The higher activity of nanofilaments relative to soot and graphite is evident. While the catalytic activity of soot decreases during the induction period because of burn-off, that of graphite and the nanofilaments increases with time. This behavior can be correlated with the stability toward combustion. Nanofilaments show a higher activity, selectivity, and yield relative to graphite. The catalytic properties of the three investigated carbon materials after 7 h operation are given in Table 1. Again the superiority of the nanofilaments over graphite is evident. Although the specific activity of nanofilaments is somewhat lower, they exhibit comparable selectivity and

[*] Prof. Dr. R. Schlögl, Dr. G. Mestl, N. I. Maksimova, Dr. N. Keller, Dr. V. V. Roddatis
Abteilung Anorganische Chemie
Fritz-Haber-Institut der Max-Planck-Gesellschaft
Faradayweg 4 – 6, 14195 Berlin (Germany)
Fax: (+49) 30-8413-4401
E-mail: Schloegl@fhi-berlin.mpg.de

[**] We thank the TIMCAL AG (Switzerland) for the generous provision of the graphite.

  1433-7851/01/4011-2066 $ 17.50+.50/0

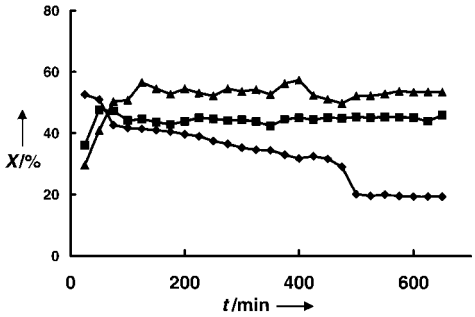

Figure 1. The styrene yield from soot (◆), graphite (■), and nanofilaments (▲) with time on stream in the oxidative dehydrogenation of ethylbenzene at 820 K.

Table 1. Comparison of the specific activities, selectivities, and yields of styrene, and the specific surface areas of lamp soot,[a] graphite, and nanofilaments after 7 h reaction.

Catalyst	Lamp soot[a]	Graphite	Filaments
Spec. activity [10^{-7} mol m^{-2}]	(14.40)	3.66	3.03
Selectivity [%]	(65)	80	85
Spec. yield [10^{-7} mol m^{-2}]	(9.32)	2.93	4.67
Spec. surface area [m^2 g^{-1}]	(19)	69	47

[a] Values in parentheses indicate that Lamp soot quantitatively combusts under the reaction conditions.

hence a 37% higher specific yield of styrene. After 7 h operation, soot still shows good performance but with extended time on stream burns up completely under these reaction conditions.

Figure 2 displays two high resolution transmission electron micrographs of nanofilament walls before and after the reaction. The fresh nanofilament walls (Figure 2a) are built

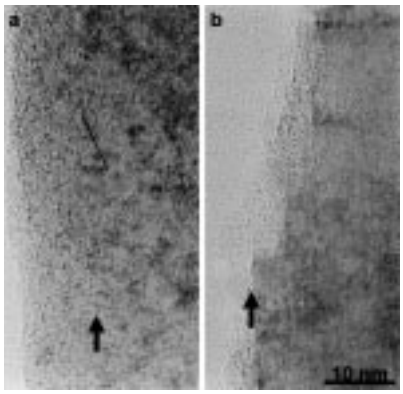

Figure 2. High resolution TEM images of the walls of carbon nanofilaments before (a) and after (b) the oxidative dehydrogenation of ethylbenzene. Arrows mark the boundary layer between the conical graphite layers and the outer shell.

up by two different layers. The inner layer is formed by conical graphite layers with an angle of 26° to the filament axis. The interlayer distance of 0.348 nm is comparable to that of normal graphite. The outer nanofilament shell is formed by ill-defined carbon layers which are oriented parallel to the filament axis. The mean layer distance is about 0.388 nm. After the catalytic reaction, the nanofilaments have an altered wall structure (Figure 2b): the outer shell of ill-defined carbon layers is combusted and a thin layer of polymeric carbon deposits covers the outer surface of the conical graphite layers. This carbon deposit can be seen especially at the step edges between the conical layers. Additionally, the ends of the conical layers seem to be partially oxidized. These partially oxidized prism faces presumably play an important role in the catalytic reaction.

The purity and composition of the test materials was characterized prior to catalysis by X-ray photoemission spectroscopy (XPS) and energy dispersive X-ray spectroscopy (EXD). The ratio of graphitic to aliphatic carbon was determined to be 0.13:1 for soot, 0.19:1 for graphite, and 0.15:1 for the nanofilaments. Hence, within the experimental error, this ratio is the same for all samples. The oxygen content was determined by EDX to be 10–20 wt% for all samples. Thus within the experimental error no difference in the oxygen content of the samples could be determined. The remaining iron-catalyst particles in the nanofilaments were always completely covered by carbon and clearly could not play an active part in the reaction.

Figure 3 displays the O(1s) XP spectrum of the nanofilament catalyst after ODH. Among others a very weak signal can be seen at 530.2 eV [17] which points to the presence of

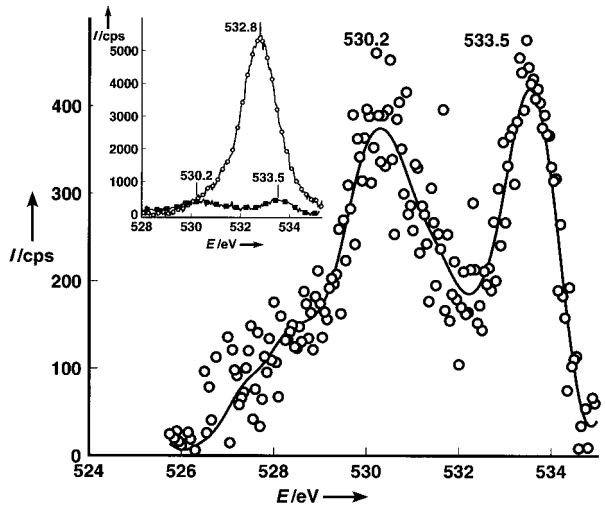

Figure 3. O(1s) XP spectrum of the carbon nanofilaments after oxidative dehydrogenation of ethylbenzene. The inset shows a comparison of the spectra before (○) and after (■) the catalytic reaction.

strongly basic surface oxygen groups,[17] for example, quinoidic groups.[18] Another weak signal at 533.6 eV is attributed to adsorbed water.[19] The detection of strongly basic groups after the catalytic reaction indicates the important dehydrogenating function these groups have during the catalytic process.

A possible reaction mechanism of the ODH of ethylbenzene over nanofilaments is shown in Scheme 1. Strongly basic, adjacent (quinoidic) oxygen centers dehydrogenate ethylbenzene to styrene under the formation of surface OH groups.[3, 9, 20] Gas-phase oxygen is dissociated on the basal planes of the graphite layers[16] and diffuses to the hydroxyl groups, which then react under reformation of the quinoidic groups and the desorption of water.

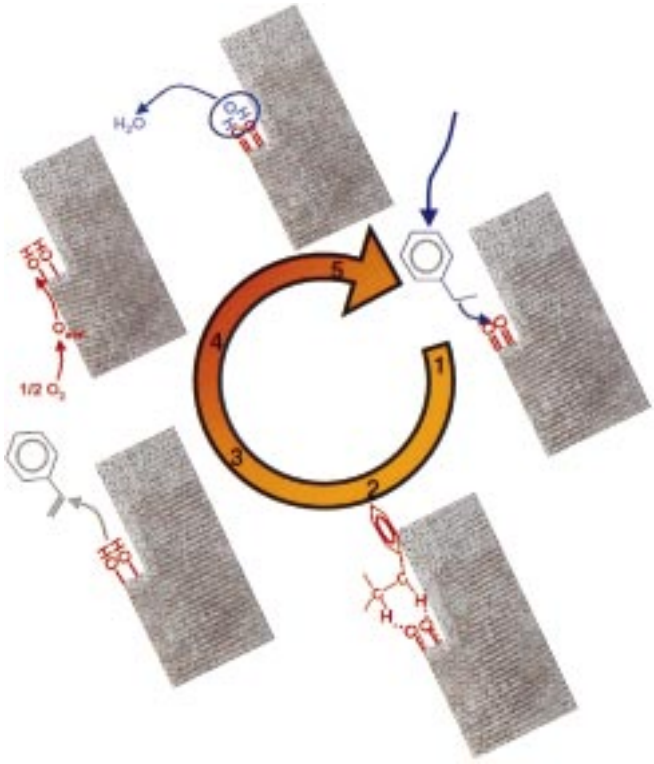

Scheme 1. Mechanism of the catalytic oxidative dehydrogenation over carbon nanofilaments, 1) adsorption of ethylbenzene, 2) dehydrogenation at basic centers, 3) desorption of styrene, 4) adsorption of oxygen and reaction with OH groups, 5) desorption of water.

Catalytic ODH giving good yields seems to be possible over carbon catalysts. Carbon nanofilaments in particular display a high stability toward oxidation; their recently reported cheap synthesis by catalytic decomposition[21] seems to make a first industrial application of carbon nanofilaments plausible. Rational design of experiments on the basis of a functional analysis of industrial catalysts with the aid of surface-science methods resulted, in a short time, in a high-temperature stable, active, and selective catalyst for the ODH of ethylbenzene.

Experimental Section

Soot (Lamp soot 101, Degussa), graphite (HSAG, TIMCAL) and commercial carbon nanofilaments (Applied Science) were used as catalysts for the oxidative dehydrogenation of ethylbenzene to styrene. The reaction was carried out in a tubular quartz reactor, inner diameter 4 mm, length 200 mm. The catalysts (0.02 g) were held in the isothermal oven zone by quartz wool plugs. He and O_2 were fed in by mass flow controllers. Ethylbenzene (EB) was evaporated at 35 °C (2.16 kPa) in a flow of He and mixed with the O_2 flow to obtain different EB:O_2 ratios (0:1, 1:1, 2:1). The reaction was carried out at 820 K in a total flow of 10 mL min^{-1} (LHSV (liquid hourly space velocity): 0.5 h^{-1}). The reaction products were analyzed on-line by gas chromatography (hydrocarbons with a 5% SP-1200/1.75% Bentone 34 packed column and flame ionization detector (FID); permanent gases with a Carboxen 1010 PLOT column/thermal conductivity detector).

The ethylbenzene conversion (X_{EB}), the styrene yield (Y_{ST}) and the selectivity to styrene (S_{ST}) were calculated according the standard reaction engineering Equations (1) – (3).

$$X_{EB} = \frac{n_{EB_{in}} - n_{EB_{ex}}}{n_{EB_{in}}} \quad (1)$$

$$S_{ST} = \frac{n_{ST}}{n_{EB_{in}} - n_{EB_{ex}}} \quad (2)$$

$$Y_{ST} = \frac{n_{ST}}{n_{EB_{in}}} \quad (3)$$

To calculate the specific activity, X_{EB} was divided by the catalyst mass and its specific surface area. The specific styrene yield was obtained analogously by dividing Y_{ST} by the catalyst mass and its specific surface area.

Transmission electron microscopy was carried out on a Phillips CM200-FEG at an acceleration voltage of 200 kV. Photoelectron spectra were recorded on a modified Leybold Heraeus spectrometer (LHS12 MCD) with $Mg_{K\alpha}$ radiation (1253.6 eV) and a power of 240 W. The bandpass energy was set to 50 eV. X-ray satellites and Shirley background was subtracted. The Brunauer – Emmett – Teller (BET) surface area of the catalysts was determined by N_2 adsorption at 77 K.

Received: December 27, 2000 [Z16326]

[1] D. H. James, W. M. Castor in *Ullmann's Encyclopedia of Industrial Chemistry*, *Vol. 25* (Eds.: B. Elvers, S. Hawkins, M. Ravenscroft, G. Schulz), 5. ed., VCH, Weinheim, **1994**, pp. 329 – 344.
[2] J. Matsui, *Appl. Catal.* **1989**, *51*, 203.
[3] F. Cavani, F. Trifiro, *Appl. Catal. A* **1995**, *133* 219.
[4] M. Muhler, R. Schlögl, G. Ertl, *J. Catal.* **1992**, *138*, 413.
[5] W. Weiss, D. Zscherpel, R. Schlögl, *Catal. Lett.* **1998**, *52*, 215.
[6] Sh. K. Shaikhutdinov, Y. Joseph, C. Kuhrs, W. Ranke, W. Weiss, *Faraday Discuss. Chem. Soc.* **1999**, *114*, 363.
[7] C. Kuhrs, Y. Arita, W. Weiss, W. Ranke, R. Schlögl, unpublished results.
[8] Z. Dziewiecki, A. Makowski, *React. Kinet. Catal. Lett.* **1980**, *13*, 51.
[9] G. Emig, H. Hofmann, *J. Catal.* **1983**, *84*, 15.
[10] G. E. Vrieland, P. G. Menon, *Appl. Catal.* **1991**, *77*, 1.
[11] G. C. Grunewald, R. S. Drago, *J. Mol. Catal.* **1990**, *58*, 227.
[12] W. Ogranowski, J. Hanuza, L. Kepinski, *Appl. Catal. A* **1998**, *171*, 145.
[13] T. G. Alkhazov, *Kinet. Katal.* **1972**, *13*, 509.
[14] M. F. R. Pereira, J. J. M. Orfao, J. L. Figueiredo, *Appl. Catal. A* **1999**, *184*, 153.
[15] M. F. R. Pereira, J. J. M. Orfao, J. L. Figueiredo, *Appl. Catal. A* **2000**, *196*, 43.
[16] R. Schlögl in *Handbook of Heteogeneous Catalysis*, *Vol. 1* (Eds.: G. Ertl, H. Knözinger, J. Weitkamp), Wiley-VCH, Weinheim, **1997**, pp. 138 – 191.
[17] H. Ago, T. Kugler, F. Cacialli, W. R. Salaneck, M. S. P. Shaffer, A. H. Windle, R. H. Friend, *J. Phys. Chem. B* **1999**, *103*, 8116.
[18] M. Voll, H. P. Boehm, *Carbon* **1971**, *9*, 481.
[19] Water is absorbed by the hydophilic groups during transfer to the XPS analysis.
[20] G. E. Vrieland, *J. Catal.* **1988**, *111*, 14.
[21] O. P. Krivoruchko, N. I. Maksimova, V. I. Zaikovskii, A. N. Salanov, *Carbon* **2000**, *38*, 1075.

  1433-7851/01/4011-2068 $ 17.50+.50/0